Available online at www.sciencedirect.com
ScienceDirect
Journal of Catalysis 254 (2008) 349–354
JOURNAL OF CATALYSIS
www.elsevier.com/locate/jcat

Promoting O_2 activation on noble metal surfaces

Wai-Leung Yim, Thorsten Klüner *

Institut für Reine und Angewandte Chemie and the Center of Interface Science (CIS), Theoretische Chemie, Carl von Ossietzky Universität Oldenburg, Carl-von-Ossietzky-Str. 9-11, 26129 Oldenburg, Germany

Received 12 December 2007; accepted 12 January 2008

Available online 11 February 2008

Abstract

We established a chemical modification strategy to search for a substitute of platinum toward O_2 activation. Achieving this required an understanding of the chemical bonding interactions along the corresponding reaction pathway. Using recently developed chemical bonding analysis schemes, we found that the transition state of O_2 dissociation on Pt(111) is stabilized by electrostatic interactions and the bonding interaction between the two oxygen atoms. This paves the way for tuning the O_2 activation barrier by replacing a surface atom with a less electronegative transition metal atom. We considered substituted Pd(111), Ag(111), and Au(111) surfaces and suggest some potential candidates for further screening by experimentalists.

Keywords: Oxygen reduction reaction; Platinum; Density functional calculations; Chemical bonding; Electrostatic interaction

1. Introduction

Due to the high cost and poor availability of platinum, extensive efforts have been made to search for a substitute in Pt-catalyzed reactions, such as oxygen reduction reactions (ORRs) [1–4]. The screening process can be facilitated by modern experimental techniques, for example, a parallel screening using scanning electrochemical microscopy (SECM) [2]. In this way, appropriate candidates can be found, although a detailed chemical understanding is beyond the scope of these experiments.

Understanding the elementary process is beneficial in efforts to improve the screening process. Although the actual environments are more complex, model studies have proven to be a promising alternative [5]. Density functional calculations are powerful for this purpose. The O_2 dissociation, a crucial step in ORR, has been studied theoretically on Pt–Co and Pt–Fe surface alloys [6], and the effect of surface strain has been investigated and rationalized by the well-known d-band model [7]. It has been suggested that alleviation of poisoning by atomic oxygen may be the reason for the active role of Pt skins (single and pure Pt layers supported by Pt–M alloy surfaces) on ORR in low-temperature fuel cells. Moreover, Fernández et al. performed a combined experimental and theoretical study to investigate the ORR on Pd–Co bimetallic alloy samples [2].

Our goal in the present work was to investigate alternatives for Pt toward O_2 activation, because of its importance in different types of reactions, like ORR and CO oxidation. The activation not only lowers the O_2 dissociation barrier, but also decreases the activity of the dissociated oxygen adatoms. Two mechanisms determine the reaction rate of ORR, O_2 dissociation and proton and electron transfer to molecular O_2 [8]. On a pure Pt surface, the strong interaction between O (or OH) and Pt limits the rate of ORR, whereas the O_2 dissociation determines the rate of ORR on Pt_3M alloy surfaces (M = Ni, Co, Fe, and Ti) [8]. Consequently, the strength of the metal–O interaction and the ease of O_2 dissociation are the two criteria for choosing possible candidates for further experimental screening.

In earlier work, Stamenkovic et al. [8] investigated Pt skins and Pt_3M alloy surfaces. Here we select a series of substituted noble metal(111) surfaces, because these surfaces are easy to handle both theoretically and experimentally using current techniques. The substituted metal surface may be synthesized by vapor deposition of a substituent element onto the M(111) surface; for example, Lahr et al. [9] prepared a sub-

* Corresponding author. Fax: +49 441 798 3964.
E-mail address: thorsten.kluener@uni-oldenburg.de (T. Klüner).

0021-9517/$ – see front matter
doi:10.1016/j.jcat.2008.01.018

stituted Au–Ni(111) surface using this well-established technique.

We performed a detailed chemical bonding analysis of a possible mechanism of O_2 dissociation on the Pt(111) surface. Knowledge of this dissociation mechanism can help guide the search for appropriate substituents. We found that the electronic structure of the transition state (TS) is influenced mainly by electrostatic effects. The scenario is similar for CO dissociation on transition metal surfaces, where Li and K act as promoters via electrostatic interactions [10–12]. This offers a way to tune the dissociation barrier. By mixing two elements of differing electronegativity, surface charges will be formed, which will decrease the energy of the TS due to electrostatic interactions. Indeed, we found that substituting a surface atom by a low-valent transition metal, such as Y, can effectively reduce the dissociation barrier compared with pure gold and silver surfaces. Based on the aforementioned criteria, we propose some potential elements.

2. Computational methods

We performed non-spin-polarized DFT calculations using the Vienna Ab Initio Simulation Package (VASP) [13–15]. We used the PBE exchange-correlation functional [16] with the PAW-projected wave function for the transition metals and the oxygen atoms [17]. The plane wave function and charge density cutoffs were set to 400 and 645 eV, respectively. We carried out geometry optimizations using the conjugate gradient minimization scheme and transition structure calculations using the climbing nudged elastic band method; the transition structures were converged to 0.07 eV/Å [18,19].

We modeled the surfaces by a slab of 4 mL thickness, exhibiting a (111) orientation. We used a (3×3) supercell containing 36 transition metal atoms. The slab images were separated by 13 Å to avoid spurious interactions between them. The bottom two layers were fixed in their optimized crystal geometry, whereas the top two layers were allowed to relax. At the alloy surfaces, one of the surface atoms was substituted. Both pure and substituted surfaces are illustrated in Fig. 1. For integration in k-space, we chose $2 \times 2 \times 1$ Monkhorst–Pack (M-P) mesh [20]. We performed convergence tests on the reaction energy and O_2 dissociation energy and found that the $2 \times 2 \times 1$ M-P mesh was sufficiently fine to obtain conclusive results, as described in Supplementary material. Details of chemical bonding analysis are also documented in Supplementary material.

3. Results and discussions

Because our goal was to investigate better alternatives for Pt toward O_2 activation, we attempted to identify elements that would have a comparable (or smaller) O_2 dissociation barrier and a weaker interaction with oxygen atoms after dissociation. Applying these search criteria, we considered the chemisorbed-O_2 precursor in an atop-hollow-bridge configuration, similar to those studied by Fernández et al. [2]. Fig. 2 schematically illustrates the O_2 precursor and dissociated oxygen adatoms on Pt(111) and AuCu surfaces. As depicted in Fig. 2A, there is one

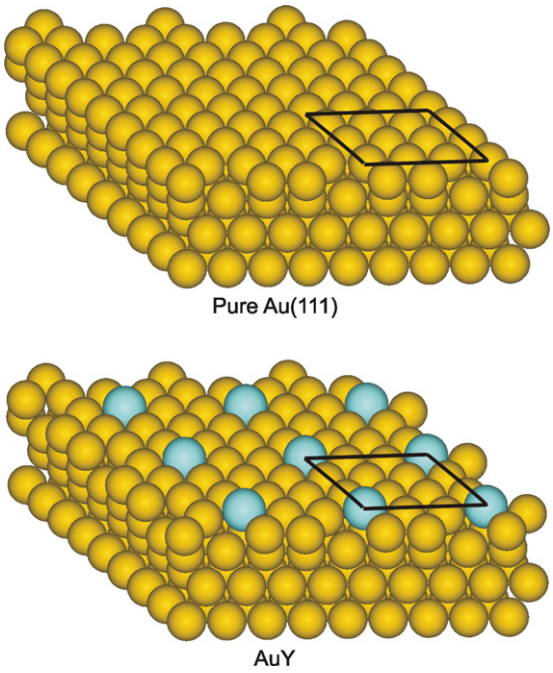

Fig. 1. Schematic diagram of pure Au(111) and AuY surfaces. The (3×3) periodic unit cells are included in the solid lines.

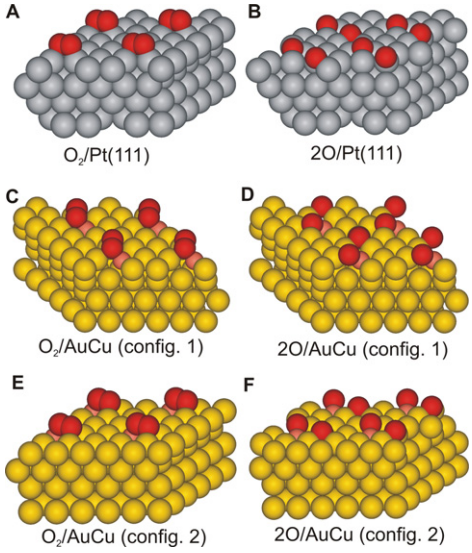

Fig. 2. Possible configurations of O_2-precursor and oxygen adatoms on: (A, B) pure Pt(111) surfaces; (C–F) AuCu alloy surfaces.

possible atop-hollow-bridge configuration for O_2 species, and the dissociated oxygen adatoms will fill the threefold hollow sites. But on the substituted alloy surfaces, such as AuCu, there are two possible atop-hollow-bridge configurations, where one oxygen can fill the Au–Cu bridge site (Fig. 2C) or the Cu-atop site (Fig. 2E). Thus, two possible dissociation channels for the chemisorbed-O_2 precursor can be identified. In this work, we studied only those O_2 dissociation pathways that exhibited the greater reaction energy on each alloy surface.

We calculated the O_2 dissociation process on the late transition metal surfaces (Table 1), including Cu(111), Pd(111), Ag(111), Ir(111), Pt(111), and Au(111). We found that the reactions on Cu(111) and Ir(111) surfaces were too exothermic,

Table 1
Energetics of O–O dissociation on late transition metal (111) surfaces, densities and Laplacian at bond critical points (BCP's)

	ΔE[a] (eV)	E_a[b] (eV)	Laplacian$_{O_2}$[c] (a.u.)		ρ_{BCP,O_2}[d] (a.u.)	
			Initial	TS	Initial	TS
Cu	−2.20	0.16	−0.14	0.36	0.28	0.13
Pd	−1.52	0.70	−0.46	0.37	0.36	0.11
Ag	−0.61	1.77	−0.46	0.09	0.35	0.03
Ir	−2.01	0.07	−0.10	0.37	0.28	0.16
Pt	−1.34	0.41	−0.34	0.20	0.33	0.06
Au	−0.21	1.25	−0.59	0.28	0.38	0.08

[a] Change of energy: $\Delta E = E[\mathrm{O(ad)}\ldots\mathrm{O(ad)}] - E[\mathrm{O_2(ad)}]$.
[b] Activation energy: $E_a = E(\mathrm{TS}) - E[\mathrm{O_2(ad)}]$.
[c] Laplacian of electron density at BCP.
[d] Electron density at BCP.

despite the low O_2 dissociation barriers. Thus, the strong O–Cu and O–Ir binding disfavors these two transition metal elements for the ORR. We did not consider these two surfaces further, because a destabilization scheme for the product states would be required to reduce the exothermicity.

We found that the O_2 dissociation on Pt(111) is exothermic by −1.34 eV, with a small barrier of 0.4 eV. As mentioned earlier, the rate of ORR on pure Pt surfaces is limited by the strong O–Pt interaction; thus, we selected a model surface that leads to a comparable O_2 activation energy and has a weaker interaction with oxygen adatoms. Among the selected late transition metal surfaces, Pd(111), Ag(111), and Au(111) fulfill the latter requirement, because the O_2 dissociation on these surfaces is exothermic by −1.52 to −0.21 eV and the surfaces are not likely to be poisoned. But the barriers are relatively large and must be decreased, especially on Ag(111) (1.77 eV) and Au(111) (1.25 eV). One possible modification would be to replace one surface atom in the topmost layer in each supercell. We discuss the choice of the substituent later.

The key to improving the ORR on Pd(111), Ag(111), and Au(111) surfaces is to reduce the large dissociation barriers. To work out a new strategy for improving catalytic performance, we obtained microscopic information of the chemical bond at the initial states and TSs on the pure Pt(111) surface. As shown in Table 2, the chemisorbed O_2 carries a net negative charge of −0.67 e. At the transition state, the O···O species is even more anionic, carrying charge of −1.12 e. Accordingly, the Pt atoms to which the O species attaches reveal an increased cationic character. The charge density can be analyzed according to a multipole expansion, which reveals that the electric monopole dominates the interaction. Thus, we can tailor the activation barrier by introducing surface charges, because the TS will be favored by electrostatics to a greater extent than the initial state. A similar situation also can be observed in O_2/Pd(111), O_2/Ag(111), and O_2/Au(111).

Table 1 also reports the electron density and its Laplacian at a bond critical point for the O_2 moiety [21]. In all cases, the chemisorbed O_2 molecule in the initial state is characterized by a covalent bond, as indicated by an average ρ_{BCP,O_2} of 0.33 a.u. and a negative Laplacian. For comparison, we analyzed the chemical bond of an isolated triplet O_2 molecule and obtained a ρ_{BCP,O_2} of 0.51 a.u. At the TS, the O–O bond is significantly weakened (small ρ_{BCP,O_2}) but remains considerable. Thus, at the precursor state, O_2 can be characterized by a strong covalent bond with a negative Laplacian at the BCP, whereas the TS reveals a polar covalent bond with a positive Laplacian at the BCP (see Supplementary material).

Table 2
Selected chemical properties for O_2/Pt(111)

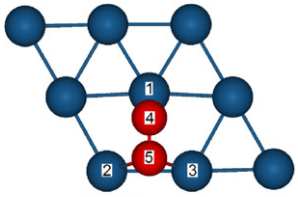

Initial structure

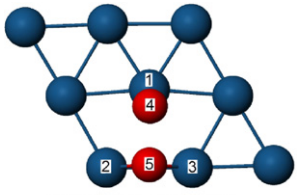

Transition structure

Atom	Charges[a] (e)	
	Initial	TS
Pt1	+0.23	+0.42
Pt2	+0.18	+0.29
Pt3	+0.17	+0.30
O1	−0.30	−0.51
O2	−0.37	−0.61
Bond	**ρ_{BCP} (a.u.)**	
Pt1–O4	0.12	0.17
Pt2–O5	0.08	0.12
Pt3–O5	0.08	0.12
O4–O5	0.33	0.06
	Laplacian (a.u.)	
Pt1–O4	0.22	0.23
Pt2–O5	0.19	0.23
Pt3–O5	0.20	0.23
O4–O5	−0.34	0.20
	E_{mono}[b] $(1/4\pi\varepsilon_0)$	
	−0.03	−0.21

[a] Atomic charges.
[b] Energy contribution by the electric monopole term.

It is noteworthy that the dissociation barrier is inversely proportional to ρ_{BCP,O_2} at the TS, except for Pt(111). Therefore, the larger ρ_{BCP,O_2} at the TS is, the smaller the dissociation barrier turns out to be.

We propose substituting a surface atom by another transition metal of different electronegativity, to enhance surface charges and in turn stabilize the TS. The topmost layer would have Pd_8M, Ag_8M, and Au_8M compositions. Substituents are selected in such a way that the chemical systems contain an even number of electrons so that non-spin-polarized calculations can be carried out. Fig. 3 shows chemical bonding information on the O–O bond at the precursor states. Both oxygen atoms carry a negative charge; the average values are illustrated in the figure. Interestingly, we observed a linear correlation between the charge of oxygen atoms and ρ_{BCP} of the O–O bonds on selected pure and substituted surfaces; the more negative the oxygen atom, the weaker the O–O bond, due to occupation of the antibonding $2\pi^*$ orbital. This supports our intuition that a substitution of electropositive atoms will increase the anionic character of the oxygen moiety and thereby weaken the O–O bond of the precursor state.

Table 3 summarizes the energetics of substituted Pd(111), Ag(111) and Au(111) surfaces. For the substituted Pd(111) surfaces, PdZn and PdRu are good candidates for O_2 activation, with activation barriers of 0.43 eV and 0.31 eV, respectively. Furthermore, the reaction energy for O_2 dissociation on these surfaces is similar to that of Pt(111). Therefore, the reaction energy profile of O_2 dissociation on Pt(111) should be mimicked by using PdZn and PdRu. On the other hand, the O_2 molecule

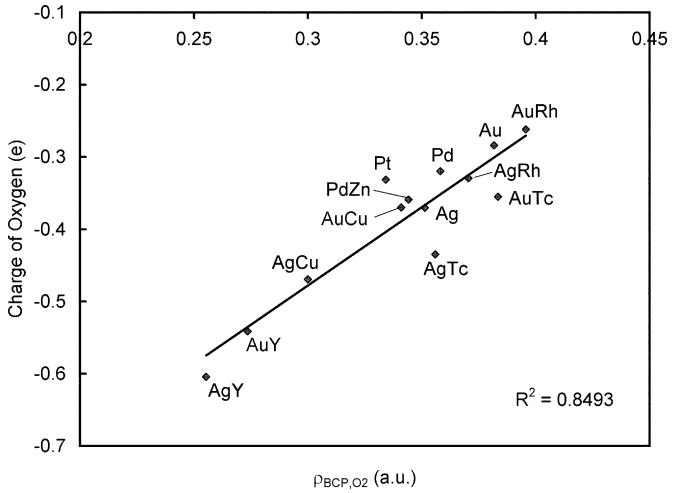

Fig. 3. Average charge at the oxygen atom as a function of ρ_{BCP} of O–O at the precursor state.

Table 3
Energetics of O–O dissociations on substituted (111) surfaces and analysis of the chemical bond of the transition state. Definitions of the quantities refer to Table 1

	ΔE (eV)	E_a (eV)	Laplacian$_{O_2}$ (a.u.)		ρ_{BCP,O_2} (a.u.)	
			Initial	TS	Initial	TS
PdTi	−1.49	0.01	0.10	0.12	0.25	0.24
PdZn	−1.59	0.43	−0.41	0.40	0.34	0.14
PdZr	−1.18	0.09	0.01	0.40	0.26	0.14
PdRu	−1.70	0.31	−0.38	−0.38	0.35	0.35
PdMo	−2.30	0.24	−0.30	0.40	0.32	0.15
AgRh	−0.38	0.86	−0.51	0.22	0.37	0.07
AgTc	−1.41	0.33	−0.41	0.42	0.36	0.13
AgNb	−0.96	0.02	−0.04	−0.06	0.27	0.27
AgY	−2.17	0.39	0.01	0.34	0.26	0.11
AgCu	−0.75	0.72	−0.23	0.21	0.30	0.06
AuRh	0.08	0.91	−0.62	0.17	0.40	0.06
AuTc	−1.23	0.32	−0.54	0.42	0.38	0.13
AuNb	−0.89	0.08	−0.04	−0.03	0.27	0.27
AuY	−1.24	0.58	−0.08	0.29	0.27	0.09
AuCu	−0.46	0.78	−0.41	0.25	0.34	0.07

dissociates immediately on PdTi and PdZr surfaces, due to the negligible barrier. This is attributed to a very strong tendency to form titanium oxide and zirconium oxide.

Our computational findings may explain the good catalytic performance of PdTi as reported by Fernández et al. [4]. With regard to the two aforementioned screening criteria, PdZr may be the best candidate for promoting ORR among the Pd series, because it leads to a tiny O_2 dissociation barrier and has a smaller reaction energy of −1.18 eV compared with pure Pt(111).

Among all substituted Ag(111) surfaces, O_2 dissociates immediately on a AgNb surface. Furthermore, the O_2 dissociation barrier is significantly reduced from 1.77 eV on Ag(111) to 0.33–0.86 eV. These smaller dissociation barriers may favor the ORR process even at room temperature. We found the activation energies in the following ascending order: AgTc ∼ AgY < AgCu < AgRh < Ag(111). This is in line with the electronegativity trend of the substituents (in Pauling units): Y(1.22) < Tc(1.9) ∼ Cu(1.9) < Rh(2.28). We also calculated the energy difference due to the electric monopole term by: $E'_{mono} = E_{mono}$ (TS) − E_{mono} (precursor), which describes the strength of the stabilization force due to electrostatic interactions. The energy contribution by electric monopoles can be estimated using the following formula [22]:

$$\text{monopole interaction:} \quad E_{el}(R^{AB}) = \frac{Q^A Q^B}{4\pi\varepsilon_0 R^{AB}}.$$

The overall energy contribution due to electric monopoles takes a summarization over the primitive supercell, where periodic boundary conditions are taken into account. The results for substituted Ag surfaces are displayed in Fig. 4A. We can see a reasonable correlation between E_a and E'_{mono}, demonstrating that the activation energy can be reduced by introducing a more electropositive transition metal atom. Among the Ag series, the AgY and AgTc surfaces lead to larger reaction energies compared with pure Pt(111), which do not fulfill the screening criteria. We note a negligible O_2 dissociation barrier on AuNb as well.

As demonstrated for the substituted Ag(111) surfaces, the substituents can effectively reduce the O_2 dissociation barrier on Au(111) surfaces to <1 eV, particularly on AuY and AuTc. The activation energies were found in the following ascending order: AuTc < AuY < AuCu < AuRh < Au(111). Thus, the substituents have the same effect on the activation energy of O_2 dissociation on both substituted Ag(111) and Au(111) surfaces. Fig. 4B shows the correlation between E_a and E'_{mono} on substituted Au(111) surfaces, demonstrating that the TS is stabilized predominantly by electrostatic interactions. Compared with pure Au(111), all of the Au–M alloys except AuRh exhibit higher reaction energies, but still lower than the corresponding energies on Pt(111). All Au alloys are suitable for further experimental screening. Note that on the AuCu alloy surface, the O_2 dissociation barrier is reduced dramatically, by 0.47 eV. This provides important insight into the recent experimental findings, in which a small amount of copper can greatly enhance CO oxidation on gold foams [23].

On the other hand, coordination effects may seriously complicate the scenario. Fig. 4C shows a linear correlation between the activation energy for O_2 dissociation and the electron density at the BCP. This implies that an early transition state, characterized by a high BCP density of the O–O moiety at the TS, favors oxygen dissociation.

The proposed model surfaces require further experimental confirmation, but at least we can evaluate the thermal stability of the substituted surfaces. Note that although the stability against the oxidation process under experimental conditions is an important issue, it is beyond the scope of the present investigation. We selected AuY, PdRu and PdZn surfaces, and carried out *ab initio* molecular dynamics calculations at 300 and 600 K. These surfaces were preheated to the desired temperature for 0.6 ps before using the longer canonical molecular dynamics simulations of about 9 ps applying a Nosé thermostat [24,25]. We found all of these systems to be thermally stable and observed no segregation reactions. The snapshots at the end of the

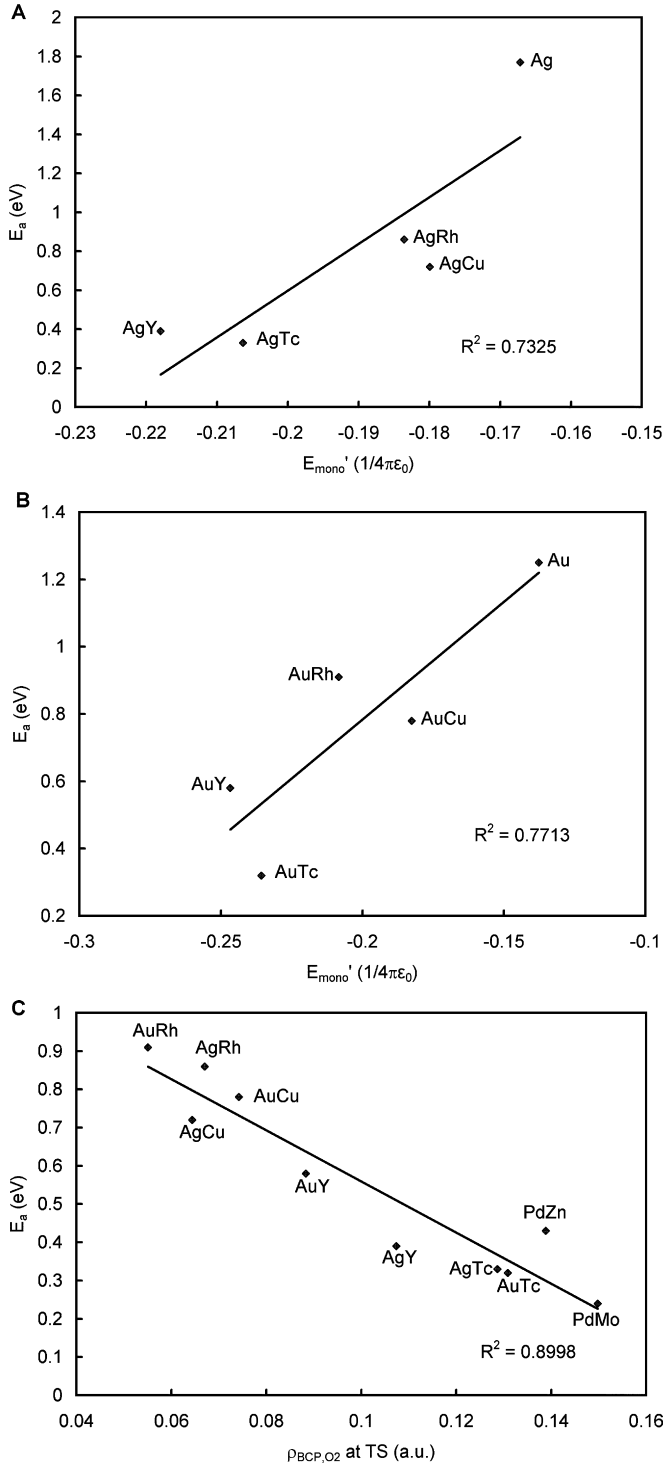

Fig. 4. (A, B) Correlation between E_a and E'_{mono}, where $E'_{\text{mono}} = E_{\text{mono}}$ (TS) $- E_{\text{mono}}$ (precursor); (C) correlation between E_a and $\rho_{\text{BCP,O}_2}$ at TS.

trajectories of the selected systems are provided in Supplementary material.

4. Conclusion

In summary, the stabilization forces due to electrostatic interaction and the subsequent weakening of the O–O chemical bond pave the way for tuning the energy barriers of O_2 dissociation. As a main result, we have identified a series of possible substitutes for Pt toward O_2 activation. Based on our two screening criteria, we suggest that PdZr, AgRh, AgNb, AgCu, AuTc, AuNb, AuY, and AuCu are good candidates for further screening by experimentalists. On these substituted surfaces, O_2 overcomes a smaller dissociation barrier, ranging from 0.02 eV to 0.86 eV. Furthermore, the reactions are unlikely to poison the surfaces, because the reaction energy ranges from −0.38 eV to −1.24 eV. Thus, for the first time, we have elucidated the underlying stabilization force for O_2 dissociation process in atomic detail by performing *ab initio* calculations. Our work may stimulate further experimental studies, especially on model systems that can effectively activate O_2 dissociation.

Acknowledgments

Financial support was provided by the Fonds der Chemischen Industrie, Alexander von Humboldt Foundation (W.L.Y.), and Hanse Wissenschaftskolleg (W.L.Y.). The simulations were performed on the national supercomputer NEC SX-8 at the High-Performance Computing Center Stuttgart under grant WLYIM.

Supplementary material

Supplementary material for this article may be found on ScienceDirect, in the online version.

Please visit DOI: 10.1016/j.jcat.2008.01.018.

References

[1] M. Nie, P.K. Shen, Z.D. Wei, J. Power Sources 167 (2007) 69.
[2] J.L. Fernández, J.M. White, Y.M. Sun, W.J. Tang, G. Henkelman, A.J. Bard, Langmuir 22 (2006) 10426.
[3] M.H. Shao, T. Huang, P. Liu, J. Zhang, K. Sasaki, M.B. Vukmirovic, R.R. Adzic, Langmuir 22 (2006) 10409.
[4] J.L. Fernández, V. Raghuveer, A. Manthiram, A.J. Bard, J. Am. Chem. Soc. 127 (2005) 13100.
[5] H.-J. Freund, M. Bäumer, J. Libuda, T. Risse, G. Rupprechter, S. Shaikhutdinov, J. Catal. 216 (2003) 223.
[6] Y. Xu, A.V. Ruban, M. Mavrikakis, J. Am. Chem. Soc. 126 (2004) 4717.
[7] B. Hammer, Y. Morikawa, J.K. Nørskov, Phys. Rev. Lett. 76 (1996) 2141.
[8] V. Stamenkovic, B.S. Mun, K.J.J. Mayrhofer, P.N. Ross, N.M. Markovic, J. Rossmeisl, J. Greeley, J.K. Nørskov, Angew. Chem. Int. Ed. 45 (2006) 2897.
[9] D.L. Lahr, S.T. Ceyer, J. Am. Chem. Soc. 128 (2006) 1800.
[10] G.A. Morgan, Y.K. Kim, J.T. Yates, Surf. Sci. 601 (2007) 3548.
[11] S.J. Pratt, D.A. King, Surf. Sci. 540 (2003) 185.
[12] M. Konsolakis, I.V. Yentekakis, Appl. Catal. B 29 (2001) 103.
[13] G. Kresse, J. Furthmüller, Phys. Rev. B 54 (1996) 11169.
[14] G. Kresse, J. Hafner, Phys. Rev. B 49 (1994) 14251.
[15] G. Kresse, J. Hafner, Phys. Rev. B 47 (1993) 558.
[16] J.P. Perdew, K. Burke, M. Ernzerhof, Phys. Rev. Lett. 78 (1997) 1396.
[17] G. Kresse, D. Joubert, Phys. Rev. B 59 (1999) 1758.
[18] G. Henkelman, H. Jónsson, J. Chem. Phys. 113 (2000) 9978.
[19] G. Henkelman, B.P. Uberuaga, H. Jónsson, J. Chem. Phys. 113 (2000) 9901.

[20] H.J. Monkhorst, J.D. Pack, Phys. Rev. B 13 (1976) 5188.
[21] R.F.W. Bader, Chem. Rev. 91 (1991) 893.
[22] F. Jensen, Introduction to Computational Chemistry, Wiley, West Sussex, 1999.
[23] V. Zielasek, B. Jürgens, C. Schulz, J. Biener, M.M. Biener, A.V. Hamza, M. Bäumer, Angew. Chem. Int. Ed. 45 (2006) 8241.
[24] S. Nosé, J. Chem. Phys. 81 (1984) 511.
[25] S. Nosé, Mol. Phys. 52 (1984) 255.